



Simulating natural carbon sequestration in the Southern Ocean: on uncertainties associated with eddy parameterizations and iron deposition

Heiner Dietze¹, Julia Getzlaff¹, and Ulrike Löptien¹

¹GEOMAR - Helmholtz Centre for Ocean Research Kiel

Correspondence to: Heiner Dietze (hdietze@geomar.de), Ulrike Löptien (uloeptien@geomar.de)

Abstract. The Southern Ocean is a major sink for anthropogenic carbon. Yet, there is no quantitative consensus about how this sink will change when surface winds increase (as they are anticipated to do). Among the tools employed to quantify carbon uptake are global coupled ocean-circulation biogeochemical models. Because of computational limitations these models still fail to resolve potentially-important spatial scales. Instead, processes on these scales are parameterized. There is concern that deficiencies in these so-called *eddy-parameterizations* might imprint wrong sensitivities of projected oceanic carbon uptake. Here, we compare natural carbon uptake in the Southern Ocean simulated with contemporary eddy-parameterizations. We find that very differing parameterizations yield surprisingly similar oceanic carbon in response to strengthening winds. In contrast, we find (in an additional simulation) that the carbon uptake does differ substantially when the supply of bioavailable iron is altered within its envelope of uncertainty. We conclude that a more comprehensive understanding of bioavailable iron dynamics will substantially reduce the uncertainty of model-based projections of oceanic carbon uptake.

1 Introduction

More than two decades after the discovery of major glacial/interglacial cycles in the CO₂-concentration of the atmosphere, it is believed that no single mechanism can account for the full amplitude of past CO₂-variability (e.g. Sigman and Boyle, 2000). There is, however, growing evidence that the variability in the extent, to which deep-water masses are isolated from the atmosphere in the Southern Ocean, is among the major drivers regulating atmospheric CO₂-variability. In this context, the role of wind-driven upwelling is of special interest (e.g. Lenton and Matear, 2007; Lovenduski et al., 2007; Marshall and Speer, 2012), especially since Anderson et al. (2009) linked increased ventilation of deep water to the deglacial rise in atmospheric CO₂.

There is also evidence that wind-driven upwelling will shape the future evolution of atmospheric CO₂-concentrations: observations during the recent decades show a strong upward trend of the dominant mode of climate variability in the Southern Hemisphere (Marshall, 2003), which is, most likely, driven by increased greenhouse gas concentrations. This upward trend of the so-called *Southern Annular Mode* is related to stronger surface winds and a pole-ward shift of the westerlies - and - is projected by climate scenarios to intensify (e.g. Simpkins and Karpechko, 2012). As to how the projected wind changes will quantitatively link to upwelling of deep waters with high carbon content (which in turn affects atmospheric CO₂-concentrations) is,



however, not comprehensively understood. The current generation of coupled ocean-circulation biogeochemical models still struggles to retrace observed trends (Lenton et al., 2013) and the models differ considerably as regards their representation of anthropogenic carbon in the Southern Ocean (Frölicher et al., 2015).

For now we know that the Southern Ocean (here defined as the region south of 40°S) accounts for more than 40% of the total annual oceanic CO₂-uptake (Takahashi et al., 2009). Further, there is evidence, based on inversions of atmospheric CO₂-concentrations (Le Quéré et al., 2007) and trends in the difference between partial pressures of CO₂ in the surface ocean and the atmosphere (Metzl, 2009; Takahashi et al., 2009) that the uptake of CO₂ in the Southern Ocean declines.

The link between strengthening winds and a declining Southern Ocean carbon sink is, however, inconclusive: global ocean-carbon models driven by observed wind patterns suggest that increased winds drive an increased exposure of carbon-rich deepwater to the surface. This leads to an overall reduced gradient between the atmosphere and the surface ocean and, subsequently, to a decreased oceanic CO₂-uptake. More specifically, all state-of-the-art coarse resolution ocean models suggest that the enhanced equatorward Ekman transport associated with a poleward shift and intensification of the southern hemisphere westerlies results in an increased circulation in the subpolar meridional overturning cell (e.g. Saenko et al., 2005; Hall and Visbeck, 2002; Getzlaff et al., 2016)). This implies an increased upwelling of deep water, rich in dissolved inorganic carbon, south of the circumpolar flow (e.g. Zickfeld et al., 2007; Lenton and Matear, 2007; Lovenduski et al., 2008; Verdy et al., 2007).

On the other hand, high resolution models that explicitly resolve eddies rather than parameterizing their effect, show that stronger westerlies induce an increased eddy activity and suggest that the associated eddy fluxes could compensate initial increases in northward Ekman transport (Hallberg and Gnanadesikan, 2006; Hogg et al., 2008; Screen et al., 2009; Thompson and Solomon, 2002). As a consequence, the upwelling, associated air-sea carbon fluxes, isopycnal tilt and the transport of the Antarctic Circumpolar Current should be rather insensitive towards changes in the wind forcing. In line with the high resolution models, observations by Argo floats do not reveal any changes in isopycnal tilt as a response to increasing winds (Böning et al., 2008). This suggests that the wind-induced upwelling can indeed be compensated by eddy fluxes.

To date, earth system models that are used to project air-sea carbon fluxes do not explicitly resolve eddy fluxes. Because of computational constraints the relevant spacial scales can not be resolved and the respective processes have to be parameterized. Typically, non-eddy resolving ocean models employ the parameterization of Gent and McWilliams (1990) (hereafter GM) to account for the effects of (unresolved) turbulent lateral advection. The "strength" of these effects in the GM parameterization is determined by a parameter, the so-called *thickness diffusivity*. In the past, for pragmatic reasons, the thickness diffusivity has been set to a globally constant value. On physical grounds, however, there is no justification for a global uniform thickness diffusivity. To the contrary, e.g. satellite observations and eddy resolving modelling clearly reveal that eddy activity varies strongly in space and time. This implies that the effect of eddies on the mean flow is inhomogeneously distributed over the ocean. Thus, recent advances have been aimed at taking the variability of the eddy field into account by parameterising the thickness diffusivity as a local function of e.g. stratification, *Eady growth rate*, or a combination of the Eady growth rate, the *Rossby radius* and the *Rhines scale*. The results of these advances towards a more realistic closure for the thickness diffusivity clearly show that mean (resolved) properties such as e.g. the simulated strength of the Antarctic Circumpolar Current or the Meridional Overturning circulation are sensitive towards the choice of the closure (Eden et al., 2009; Viebahn, 2010). This



suggests that the simulated upwelling of deep carbon-rich waters in the Southern Ocean may as well be sensitive to the choice of the closure.

In the present study, we test differing closures for GM's thickness diffusivity in a global coarse-resolution coupled ocean-circulation biogeochemical model (which comprises carbon). The focus is on how the closures will affect the sensitivity of carbon uptake in response to increasing winds in the Southern Ocean. To this end, we will revisit the apparently discrepant responses to trends in the Southern Annular Mode of (1) coarse resolution models on the one hand, and (2) eddy-resolving models and observations on the other hand.

In order to put our results concerning uncertainties associated with physical processes into perspective, we compare it with the uncertainty that is associated with incomprehensively-understood deposition of bioavailable iron.

The following Section 2 describes our global coupled ocean-circulation biogeochemical model configurations and the respective simulations. The subsections 2.2.1 and 2.2.1 give a short introduction to eddy-parameterizations and iron, respectively. In Section 3 we compare all simulations with one another. The focus is on the simulated carbon uptake of the Southern Ocean and related processes. The paper ends with a conclusive summary in Section 4.

2 Model

This study is based on simulations with the Modular Ocean Model (MOM), version MOM4p1. Specifically we use the ocean-ice component of the CM2Mc configuration coupled to the Biology Light Iron Nutrients and Gasses (BLING) ecosystem model of (Galbraith et al., 2010). We force with climatological atmospheric conditions (*Normal Year Forcing* of Large and Yeager (2004)). Our configuration is identical to the one used and described in Galbraith et al. (2010).

The nominal zonal resolution is 3° . The meridional resolution varies from 3° in mid-latitudes to $2/3^\circ$ near the equator. Additional regions of enhanced meridional resolution are the latitudes of the Drake Passage and respective latitudes on the northern hemisphere. In the Arctic, a tri-polar grid is applied to avoid discontinuities at the North Pole (c.f. Griffies et al., 2005). The vertical discretisation comprises 28 levels with a resolution ranging from 10 m at the surface to 506 m at depth.

In total we perform three 1000 year-long model spin-ups: one that is identical to the configuration described in Galbraith et al. (2010), and yet another two that differ - as we will elaborate on in Section 2.1 - as regards the parameterization of unresolved eddies (i.e. thickness diffusivity, - after Gent and McWilliams, 1990). All three spin-ups start from the semi-equilibrated state of Galbraith et al. (2010). In all simulations the atmospheric CO_2 -concentration is prescribed to a pre-industrial level of 278 ppmv. This choice of oceanic carbon boundary conditions is often applied to study the oceanic uptake of *natural* (as opposed to anthropogenic) carbon uptake (e.g. Lovenduski et al., 2007). The results from the spin-ups are evaluated in appendix A.

Each of the three spin-ups is extended in order to assess the sensitivity of simulated natural carbon uptake in the Southern Ocean towards anticipated wind changes. In each of the extensions the magnitude of the wind speeds south of 40°S is increased by a rate of 14% in 50 years. This increase is consistent with results from reanalysis for the period 1958 to 2007 (Lovenduski et al., 2013).



In the remainder of this Section we describe our sensitivity experiments in more detail. These experiments explore the impact of differing eddy parameterizations and compare it to uncertainties that are related to biogeochemical responses to changes in air-sea deposition of bioavailable iron. Tab. 1 summarizes the experimental setup. The following sub-section are organized as follows:

- 5 – Section 2.1 starts with an overview of approaches to parameterize the effect of eddies in coarse resolution models (Section 2.1.1), followed by an explicit description of our model setups and the respective simulations with differing eddy-parameterizations in Section 2.1.2.
- Section 2.2 starts with an overview of the effects of iron on primary production and associated carbon sequestration (Section 2.2.1), followed by an explicit description of our simulation with altered supply of bioavailable iron to the
 10 ocean in Section 2.2.2.

2.1 Eddy parameterizations

2.1.1 Introduction

The simulation of oceanic motion (driven by pressure gradient force, gravity and viscous friction) by numerically solving the *primitive equations* is intimately coupled to the question of how to proceed with sub-grid processes that can not be resolved but
 15 are known to affect processes on the resolved scales. The reason is that computational costs and constraints render it typically impossible to resolve all spatial scales that are involved in the dynamics of interest.

For global ocean-circulation models, that are coupled to biogeochemical (carbon) models, the explicit resolution of mesoscale processes has - so far - been already beyond computational capacities. Hence, to-date, model-based projections of oceanic carbon uptake rely on parameterizations of mesoscale processes.

20 Historically, attempts to parametrize mesoscale processes in ocean models started with relatively simple, horizontal, down-gradient *Laplacian* diffusion with associated constant diffusivities of the order of $1000 \text{ m}^2 \text{ s}^{-1}$. Early on, it has been realised by Veronis (1975) that the associated horizontal mixing results in too intense diapycnal mixing in regions of sloped isopycnals (cf. McDougall and Church, 1985). As a workaround Redi (1982) proposed to transform the horizontal diffusion tensor such scalars and momentum are mixed only along isopycnals. The conundrum with this so-called *isopycnal mixing* scheme, however, is that
 25 it (wrongly) implies that eddies do not have any effects on the dynamics in regions where the density distribution is governed by either temperature or salinity only.

To-date, virtually all climate models apply the parameterization of Gent and McWilliams (1990) (hereafter GM) to account for the effects of unresolved ocean eddies. GM constitutes a positive definite sink of the global potential energy by introducing a purely adiabatic extra advection. The parameterization is also referred to as *thickness diffusion* (even though its inventors now
 30 consider the term to be misleading; Gent, 2011) which vividly describes the effect of thickness diffusion on layers bounded by two isopycnals – that is, evening out local differences in layer thickness. Associated to GM is a parameter, often dubbed *thickness diffusivity*, or κ , which prescribes the speed with which differences in isopycnal layer thicknesses are evened out. It



is agreed that κ should be spatially varying in order to account for the fact that eddy-activity is not homogeneously distributed over the globe. But as concerns how it should or could be calculated in a coarse resolution model, there is no consensus.

The most pragmatic choice is setting κ constant (cf. Gent et al., 1995). Other approaches include " ... an attempt to tune away model bias, rather than an attempt to make a poorly represented process more physical ..." (Gnanadesikan et al., 2005),
 5 or are calibrated with results from eddy-resolving models (Eden and Greatbatch, 2008).

2.1.2 Sensitivity experiments - thickness diffusivities

The choice of the thickness diffusivity closure has been shown to cause local effects in the Southern Ocean such as differing Antarctic Circumpolar Current transports (Eden et al., 2009), and differing sensitivities of the meridional overturning circulation (MOC) towards wind stress changes (Viebahn, 2010). The question which closure yields the most realistic results has not
 10 been unanimously answered yet because the rather strong bias in all of the simulations renders comparisons to observations inconclusive. As regards simulated MOC changes in response to changing winds, there is some guidance from intercomparison with eddy-resolving models (cf. Viebahn, 2010). This guidance, however, is based on the assumption that eddy-resolving models are realistic, albeit they are - as well - biased.

Our aim here is to quantify the uncertainty in the uptake of natural carbon in the Southern Ocean that is associated to the
 15 choice of the closure for thickness diffusivity in a global coupled ocean circulation biogeochemical model. To this end, we compare results from three contemporary closures for the thickness diffusivity κ dubbed *CON*, *FMCD*, *E&G*:

- *CON*; closure is constant in space and time: $\kappa = 600 \text{ m}^2 \text{ s}^{-1}$.
- *FMCD*; closure is a function of space (longitude, latitude, tapering to the bottom and the surface) and time as a function of the horizontal density gradient averaged from 100 to 200 m depth:

$$20 \quad \kappa = \alpha |\overline{\nabla_z \rho}|^z \left(\frac{L^2 g}{\rho_0 N_0} \right). \quad (1)$$

The dimensionless $\alpha = 0.07$, the length scale $L = 50 \text{ km}$, and the Brunt-Väisälä frequency $N_0 = 0.004 \text{ s}^{-1}$ are tuning constants. $g = 9.8 \text{ m s}^{-2}$ is the standard acceleration of free fall. $\rho_0 = 1035$ is the reference density for the Boussinesq approximation and $|\overline{\nabla_z \rho}|^z$ is the average of the horizontal density gradient taken over the depth range 100 to 2000 m. Maximum and minimum values are set to 2000 and $200 \text{ m}^2 \text{ s}^{-1}$, respectively.

- *E&G*; closure is a function of space (longitude, latitude, depth) and time as proposed by Eden and Greatbatch (2008) based on considerations of the eddy kinetic energy budget:

$$25 \quad \kappa = L^2 \sigma, \quad (2)$$

where the inverse time scale $\sigma = |\partial_y \bar{b}|/N = |f \partial_z \bar{u}|/N$ is related to the Coriolis parameter f , the vertical shear of the mean flow $\partial_z \bar{u}$ and the Brunt-Väisälä frequency N . σ is also referred to as the Eady growth rate which is a measure of
 30 the baroclinic instability. The length scale L is set as $L = \min(L_R, L_{Rhi})$, with the local first baroclinic Rossby radius



L_R and the Rhines Scale $L_{Rhi} = \sqrt{u/\beta}$. The Rhines Scale defines the spatial scale at which planetary rotation causes zonal jets. It is a function of the eddy horizontal velocity u and β (the latitudinal gradient of f).

In addition to the thickness diffusivities discussed above we apply an isopycnal diffusivity of $600 \text{ m}^2 \text{ s}^{-1}$ in all configurations presented here.

5 2.2 Iron deposition

2.2.1 Introduction

Iron, although an abundant element on earth, is present only at very low concentrations in the ocean. Typically, the vertical distribution shows a profile which is similar to nitrate or phosphate (e.g. Johnson et al., 1997), with lower concentrations at the surface ($< 0.2 \text{ nmol kg}^{-1}$) and concentrations peaking further down in the thermocline (at around 1 nmol kg^{-1}). Another
10 similarity to nutrients like nitrate or phosphate is that in vast oceanic regions, the growth of autotrophs is limited by the availability of iron (cf. Boyd and Ellwood, 2010). Among the iron-limited regions is the Southern Ocean where direct observational evidence shows that changes in iron supply affect the biotic uptake of carbon and its export to depth (Smetacek et al., 2012).

To this end a consensus has been reached in the literature. The global oceanic iron cycle is an important agent in the global biogeochemical carbon cycle. But, even so, there is still a large discrepancy between the evidential importance of iron
15 dynamics and our poor quantitative understanding thereof. One expression of this discrepancy is that, on the one hand, the biogeochemical protocols for the CMIP6 Ocean Model Intercomparison Project (cf. Eyring et al., 2016) now rank simulated dissolved iron concentration as "priority 1" model output (Orr et al., 2016, their Table 5) while, on the other hand, the same protocols suggest not to initialize the models with observations of dissolved iron because suitable data compilations are not available yet.

20 In short, neither sources nor sinks of dissolved iron in the ocean are well constrained and data of standing stocks are so sketchy that the scientific community recommends not to use these data for simulations. Among the reasons for this dire situation are challenges such as (1) sources and sinks overlap spatially such that standing stocks of iron can not constrain the (speed of the) iron cycling (Frants et al., 2016), (2) aeolian sources of iron are intermittent and thus hard to quantify (e.g. Duggen et al., 2010; Olgun et al., 2011), (3) physico-chemical stabilization is not well understood such that e.g. the importance
25 of iron originating from hydrothermal vents remains uncertain (Resing et al., 2015), and (4) iron sinks such as scavenging and precipitation are not well constrained (e.g. Tagliabue et al., 2014) and an explicit representation of the essential iron-binding ligand dynamics in models has only just begun (Völker and Tagliabue, 2015).

2.2.2 Sensitivity experiment - iron supply

The cycling of iron in the ocean is not well constrained: in terms of an average residence time, contemporary models differ by
30 two orders of magnitudes (4 to 600 years Tagliabue et al., 2016). It is straightforward to assume that the large uncertainty in the supply and cycling of iron affects the sensitivity of simulated oceanic carbon uptake. As a first step towards relating uncertainties in iron dynamics with oceanic carbon uptake we conduct a sensitivity experiment were we change the aeolian supply



of bioavailable iron to the ocean. (Note that, to fathom the full range of uncertainty is beyond the scope of this manuscript.)
 The ratio behind this experiment is as follows: in a warming world the amount of dust air-borne is increasing due to vegetation
 loss, dune remobilization (e.g., Bhattachan et al., 2012) and glacier retreat (e.g., Bullard, 2013). In-line with this reasoning,
 model-aided estimates by Mahowald et al. (2010) suggest that the increase may well correspond to a doubling over the 20th
 5 century over much of the globe. In our experimental design, we follow Krishnamurthy et al. (2009) and assume in our sensitiv-
 ity experiment *IRON* that the deposition of bioavailable iron, associated to aeolian dust, does also double over a period of 50
 years. Other than these changes of iron supply, the simulation *IRON* is identical to the simulation *FMCD*.

Simulation Tag	Description
CON	The model configuration is identical to Galbraith et al. (2010) but with a constant thickness/eddy diffusivity of $600 \text{ m}^2 \text{ s}^{-1}$. Starting from the semi-equilibrated state of Galbraith et al. (2010), we continue the spin-up by another 20 years, after which we increase the windspeed that drives the ocean south of 40°S . The respective increase is 14% in 50 years, consistent with results from a reanalysis of the period 1958 to 2007 (Lovenduski et al., 2013).
FMCD	The model configuration and integration procedure is identical to CON except for the eddy parameterisation which is set to the default CM2.1 setting in Galbraith et al. (2010) with a spatially varying thickness diffusivity.
E&G	The model configuration and integration procedure is identical to CON except for the eddy parameterisation which is set to spatially-varying following Eden and Greatbatch (2008) in its simplified form of Eden et al. (2009).
IRON	The underlying model configuration and integration procedure is identical to FMCD except for air-sea fluxes of iron south of 40°S which are increased by a rate corresponding to a doubling in 50 years.

Table 1. Model simulations.



3 Results

Fig. 1 and Fig. 2 show thickness diffusivities in the configurations FMCD and E&G at the end of their spin-up: we find a $\approx 40\%$ difference in the average diffusivities between the contemporary concepts FMCD, E&G and the constant value of $600\text{m}^2\text{s}^{-1}$ in CON.

- 5 The thickness diffusivities in both FMCD and E&G vary substantially in space (Fig. 1) although not in unison: in FMCD we find large thickness diffusivities in the region of the Antarctic Circumpolar Current (ACC), which is in line with results from high resolution models and observations (e.g. Frenger et al., 2013; Hallberg and Gnanadesikan, 2006). In E&G the elevated values in the ACC are less pronounced and elevated diffusivities appear in the Weddell and Ross sea. In E&G, in contrast to FMCD, even the large values decay rapidly with depth (Fig. 2). Both FMCD and E&G peak locally at values twice as large
10 as the constant thickness diffusion applied in CON (Fig. 1). Even so the zonal averages of FMCD and E&G are typically lower than in CON (Fig. 2). The thickness diffusivities vary not only substantially among the configurations at the end of the respective spin-ups, but they do also feature differing sensitivities towards increasing winds. While the thickness diffusivities in CON stay constant at $600\text{m}^2\text{s}^{-1}$, the thickness diffusivities in both, FMCD and E&G, show a similar – albeit not identical – pattern of increase (Fig. 3a and b). Expressed in terms of a thickness diffusivity averaged over the whole Southern Ocean
15 the increase is linearly related to the wind increase and peaks at 16 and $25\text{m}^2\text{s}^{-1}$ in the configurations E&G and FMCD, respectively (Fig. 3c).

In the following, we summarize the oceanic responses to the combination of increasing winds and changing thickness diffusivities:

- Ekman pumping. The vertical velocities that are driven by the horizontal divergence of Ekman transports increase along
20 with the winds by up to 50m yr^{-1} (Fig. 4). The responses of all considered configurations are almost identical (i.e. indistinguishable by eye), indicating that surface current/wind effects (cf. Dietze and Löptien, 2016) differ very little among the configurations. This also indicates that the kinetic energy transferred from the atmosphere to the ocean is very similar in all of the configurations.
- Meridional overturning. In all configurations the increased winds drive an enhanced meridional overturning with similar
25 patterns and amplitudes (Fig. 5). Also common to all configurations is that the fraction of meridional overturning that is effected by the respective GM parameterization is opposing the increasing trend (i.e. the changes in Fig. 6 are negative over most of the region). The magnitude of this counter effect, however, differs considerably among the configurations. Fig. 6 reveals that the counter effect, or "eddy compensation" as it is also referred to, peaks at 2 Sv in CON and E&G while FMCD features much higher values up to 4 Sv. Note that these results do not support the hypothesis that a more
30 complex definition of the thickness diffusivity (such as in E&G and FMCD) does necessarily amount to an increase of the (parameterized) eddy compensation relative to the original pragmatic choice (cf. Gent et al., 1995) of setting it constant (such as in CON).



- Air-sea heat flux. The air-sea heat flux averaged over the Southern Ocean is an indicator of diabatic heatfluxes in its thermocline. After all heat exchanged between the surface mixed layer and the atmosphere has to be replaced from somewhere. (This view neglects trends in sea surface temperature and near-surface oceanic heat fluxes entering the region). Fig. 7a shows the temporal evolution of heat exchanged with the atmosphere. The most striking feature is that in all configurations the air-sea heat exchange is relatively constant, even though the winds increase considerably. Other than that, there is a small offset between the configurations, indicating differences in the meridional overturning of heat. Short term anomalies in time, such as between year 30 and 40 in FMCD and E&G in Fig. 7a, are correlated with sea-ice extent.
- Sea ice cover. Among the biggest concern in preparation of the configurations was sea ice. The reason is that sea ice caps the ocean shielding it from air-sea exchange of heat and carbon. Thus, sea-ice dynamics is coupled to carbon uptake and a comparison of model configurations that feature differing sea-ice covers can be challenging. The intimate coupling between sea-ice cover and air-sea fluxes is evident in Fig. 7a and b. All anomalies in the heat fluxes (such as e.g. between year 30 and 40 in E&G and FMCD) have their counterpart in sea ice extent, suggesting that less sea-ice results in more cooling of the ocean as vaster areas of relatively warm ocean waters are exposed to the cold polar atmosphere. Fortunately, the temporal evolution of sea ice extent is very similar among the configurations. If it were not (such as e.g. in the configurations compared by Bryan et al., 2014), the interpretation of results would not be straightforward.

Despite some significant differences in simulated physics among the configurations FMCD, E&G and CON (such as, e.g., differing levels of eddy-compensation) the simulated differences in oceanic carbon uptake are small (Fig. 7c). So small that we conclude that the simulated oceanic carbon uptake in the Southern Ocean is rather robust towards the choice of details in the contemporary eddy-parameterization of Gent and McWilliams (1990). In each of our configurations FMCD, E&G and CON the carbon uptake of the Southern Ocean decreases almost linearly in time. Eventually, the Southern Ocean turns from a sink to a source of natural carbon, irrespective of the eddy-parameterization. Other than that there are small deviations from a linear decrease such as e.g. the "anomaly" between year 60 and 70 in configuration CON. These deviations correspond to changes in ice extent with less sea ice being associated with stronger outgassing (or less uptake) of carbon.

A similarly robust behaviour is, however, not inherent to biogeochemical module. By changing the deposition of bioavailable iron within its "envelope of uncertainty" in experiment IRON the oceanic carbon uptake does change substantially. Fig. 7 shows that even the sign of air-sea carbon fluxes in the Southern Ocean changes relative to all the other simulations.

4 Summary and conclusion

Global coupled ocean-circulation biogeochemical models predict an increase of oceanic natural CO₂-outgassing due to strengthening winds in the Southern Ocean (e.g. Lovenduski et al., 2013). These predictions contain a considerable degree of uncertainty, some of which that is associated to what Lovenduski et al. (2016) refer to as inter-model "structural differences".

In the present study, we compare two sources of uncertainties in simulated carbon uptake in response to increasing winds in the Southern Ocean with one another: (1) The uncertainty related to actively discussed details in the contemporary (GM-)



parameterization of Gent and McWilliams (1990) which mimics the effects of unresolved mesoscale circulation on the resolved larger scale circulation in coarse resolution models. Specifically, we explore different definitions of the respective thickness diffusivity. (2) To put the results into perspective, we also consider the uncertainty that is related to the rather unconstrained deposition of bioavailable iron to the sun-lit surface ocean.

5 The investigation of the GM-parameterization is motivated by studies such as of Farnetti and Gent (2011); Gent and Danabasoglu (2011), who argue that a variable, rather than a constant, thickness diffusivity is key to a realistic effect of unresolved mesoscale physical processes on the resolved (coarse resolution) circulation that - in turn - is an essential precondition for a realistic response of the Southern Ocean to stronger winds. Lovenduski et al. (2013) support this view and find, indeed, that the sea-air CO₂-outgassing is damped by (parameterized) eddy compensation in scenarios with strengthening winds. To
 10 this end, our results based on a suite of model simulations are consistent in that they also show an eddy compensation that significantly dampens the increase of the meridional overturning circulation in response to increasing winds. As regards the magnitude of the response on air-sea carbon fluxes we find, however, that differences between contemporary approaches to define the thickness diffusivity of Gent and McWilliams (1990) are small. Or, in other words, GM's eddy-parameterization is relatively robust towards the choice of the respective scaling coefficient (i.e. the thickness diffusivity). In our opinion this
 15 enhances the credibility of GM's seminal parameterization. This is fortunate because a high sensitivity towards the choice a scaling coefficient would not be a good base for a projection of oceanic carbon uptake in a warming world.

In contrast, our results indicate that the biogeochemical module tested here, does not yet feature a robust response. Specifically we explored the uncertainty that is associated with the air-sea deposition of bioavailable iron which - on its own - prevents the specification of even the sign of air-sea carbon fluxes in a world of increasing winds. Note that the overall uncertainty due
 20 to the biogeochemical component must be much higher as not only the iron supply tested here is uncertain, but also, the residence time of iron varies by two order of magnitudes among contemporary biogeochemical models (Tagliabue et al., 2016). Additional uncertainty is associated with the Michaelis-Menten formulation - a concept which is generic to biogeochemical modelling and which describes the limitation of autotrophic growth whenever essential resources (such as iron) are depleted. Although the Michaelis-Menten formulation is generic it is discussed controversially. Developed with enzyme kinetics in mind
 25 it may not be applicable to autotrophs (e.g., Smith et al., 2009), and respective parameters (so-called half saturation constants) may be impossible to constrain with typical observations (Löptien and Dietze, 2015), even though they exert crucial control on the models' solutions.

In summary, our results indicate that a poor quantitative understanding of biogeochemical processes is a major source for uncertainties in model-based estimates of oceanic uptake of natural carbon in the Southern Ocean. Ranked against uncertainties
 30 associated with the choice of the thickness diffusivity, the impression is that uncertainties in biogeochemical processes dominate. Given that the biogeochemical modules, in contrast to the physical modules, are not build based on first principles (such as Newton's Laws) this may not be astounding. Note, however, that there are regions where the opposite hold: e.g. findings by Dietze and Löptien (2012) suggest that an incomprehensive understanding of physical rather than biogeochemical processes prevents a realistic modelling of biogeochemical processes in the thermocline of the eastern tropical Pacific.



A caveat remains. Although we showed that GM's parameterization is, in terms of the carbon uptake in the Southern Ocean, rather robust - still - all of our coarse-resolution simulations could be biased. To this end, the increase in computer power is about to provide some guidance now that recent configurations can afford to resolve much of the mesoscale (e.g. Dufour et al., 2015; Bishop et al., 2016) in the Southern Ocean - albeit they have no explicit representation of the carbon cycle yet. Hence a comparison of the sensitivity of carbon uptake to increasing winds between coarse resolution models (like the configurations tested here) and configurations that explicitly resolve mesoscale processes, is to come. For the time being Gent (2016) summarizes the respective field of physics-only configurations by stating that high-resolution models have approximately 50% compensation of the MOC-increase. Thus, all the simulations shown here may underestimate the eddy compensation by a factor of two.

10 Appendix A: Model assessment

A comprehensive evaluation of the spun-up configuration FMCD is provided by Galbraith et al. (2010) who show that the model is competitive in the sense that its deviations from observations is similar to what can be expected from the current generation of earth system models. Here, we show a small choice of model-data comparisons only:

- Sea surface temperature (SST, Fig. 8) is associated to oceanic carbon storage via the solubility of water that is in contact with the atmosphere. Further, SST biases are indicative of deficient physics in setups like ours, where SST is not restored but effected by the entanglement of air-sea heat fluxes with ocean circulation.
- Surface phosphate concentrations (Fig. 9) are indicative for the efficiency of the biological carbon pump to draw down surface nutrients which are continuously re-supplied to the sun-lit surface by upwelling and vertical diffusive processes.
- Zonally averaged meridional section of oxygen concentrations (Fig. 10) are indicative for the balance between deep ocean ventilation and biotic oxygen consumption.
- Sea ice cover (Fig. 11) is supposedly, according to e.g. Bryan et al. (2014), key to simulated air-sea carbon fluxes as it can cap the air-sea exchange of gases. Note that all of our simulations feature very similar ice cover (which is not shown explicitly here, but indicated by the similar ice extent in Fig. 7 c).

Closer inspection of Fig. 8 to 11 reveals typical model deficiencies, among them (1) a SST cold bias (Fig. 8) in the eastern tropical Pacific and Indic, (2) a spurious nutrient drawdown in oligotrophic regions (Fig. 9) which may be the consequence of a wide-spread, but flawed, phytoplankton growth concept (Smith et al., 2009), (3) an equatorial oxygen deficit (Fig. 10) which is related to unresolved physics (Dietze and Löptien, 2012; Getzlaff and Dietze, 2013), (4) an oxygen distribution which is biased high polewards of 60°N and close to Antarctica which is probably associated with deficient deep water formation, (5) overestimated sea ice melting in Summer around Antarctica (as can be derived from Fig. 11).

Here we conclude that all of our semi-equilibrated model configurations (listed in Tab. 1) feature simulations that deviate by roughly equal amounts from the observations. This, in its turn, suggests that the simulated sensitivities of any of our



configurations towards changing winds in the Southern Ocean, is equally likely. Or in other words, none of our simulations can be discarded nor favoured with the argument that the respective simulated mean state is especially unrealistic or realistic.

Author contributions. All authors were involved in the design of the work, in data analysis, in data interpretation and in drafting the article.

Acknowledgements. Eric Galbraith, contributor to the MOM (www.gfdl.noaa.gov/mom-ocean-model/) community and developer of BLING
5 (www.sites.google.com/site/blingmodel/), shared his model configuration with us. We are grateful to him and the rest of the MOM community! All authors acknowledge long-term support by Andreas Oschlies. J. G. acknowledges funding by *Deutsche Forschungsgemeinschaft* via the project "Impact of eddy parameterisations on the simulated response of Southern Ocean air-sea CO₂-fluxes to wind stress changes in IPCC-type ocean models". Integrations were performed on the compute clusters weil.geomar.de, wafa.geomar.de, and other hardware from the GEOMAR Helmholtz Centre for Ocean Research, Germany, Kiel, FB2/BM. Further, we used the scalar HPC cluster of the NEC System
10 at the Christian-Albrechts-Universität zu Kiel which is co-funded by GEOMAR. The authors wish to acknowledge use of the Ferret program for analysis and graphics in this paper. Ferret is a product of NOAA's Pacific Marine Environmental Laboratory. (Information is available at <http://ferret.pmel.noaa.gov/Ferret/>)



References

- Anderson, R. F., S. Ali, L. I. Bradtmiller, S. H. H. Nielsen, M. Q. Fleisher, B. E. Anderson and L. H. Burckle (2009). Wind-driven upwelling in the Southern Ocean and the deglacial rise in atmospheric CO₂, *Science*, 323(5920), 1443–1448, doi: 10.1126/science.1167441.
- Bishop, S. P., Gent, P. R., Bryan, F. O., Thompson, A. F., and R. Abernathy (2016). Southern Ocean Overturning Compensation in an
5 Eddy-Resolving Climate Simulation, *J. Physical Oceanography*, 46, 1575–1592, doi: 10.1175/JPO-D-15-0177.1.
- Böning, C. W., A. Dispert, M. Visbeck, S. R. Rintoul and F. U. Schwarzkopf (2008). The response of the Antarctic Circumpolar Current to recent climate change, *Nature Geoscience*, 1, 864–869, doi: 10.1038/ngeo362.
- Bhattachan, A., D'Odorico, P., Baddock, M.C., Zobeck, T.M., Okin, G.S. and N. Cassar (2012). The Southern Kalahari: a potential new dust source in the Southern Hemisphere? *Environmental Research Letters*, 7, doi: 10.1088/1748-9326/7/2/024001.
- 10 Boyd, P. W., and M. J. Ellwood (2010). The biogeochemical cycle of iron in the ocean, *Nature Geoscience*, 3, 675–682, doi: 10.1038/ngeo964.
- Bullard, J.E. (2013). Contemporary glacial inputs to the dust cycle, *Earth Surface Processes and Landforms*, 38, doi: 10.1002/esp.3315.
- Bryan, F.O., Gent, P.R. and R. Tomas (2014). Can Southern Ocean eddy effects be parameterized in climate models?, *J. Climate*, doi:10.1175/JCLI-D-12-00759.1.
- Dietze, H. and U. Löptien (2012). Revisiting "nutrient trapping" in global coupled biogeochemical ocean circulation models, *Glob. Bio-geochem. Cycles*, 27, doi: 10.1002/gbc.20029.
- 15 Dietze, H. and U. Löptien (2016). Effects of surface current/wind interaction in an eddy-rich general ocean circulation simulation of the Baltic Sea, *Ocean Science*, 12, 977–986, doi:10.5194/os-12-977-2016.
- Duggen, S., Olgun, N., Croot, P., Hoffmann, L., Dietze, H., Delmelle, P., and C. Tescher (2010). The role of airborne volcanic ash for the surface ocean biogeochemical iron-cycle: a review, *Biogeoscience*, 7, 827–844, doi: 10.5194/bg-7-827-2010.
- 20 Dufour, C. O., S.M. Griffies, G. F. de Souza, I. Frenger, A.K. Morrison, J. B., Palter, J. B., J.L. Sarmiento, E.D. Galbraith, J.P. Dunne, W.G. Anderson and R.D. Slater (2015). Role of mesoscale eddies in cross-frontal transport of heat and biogeochemical tracers in the Southern Ocean. *J. Physical Oceanography*, 45(12), 3057–3081, doi: 10.1175/JPO-D-14-0240.1.
- Eden, C. and R. Greatbatch (2008). Towards a mesoscale eddy closure; *Ocean Modelling*, 20, 223–239, doi: 10.1016/j.ocemod.2007.09.002.
- Eden, C., M. Jochum, and G. Danabasoglu (2009). Effects of different closures for thickness diffusivity, *Ocean Modelling*, 26, 47–59, doi: 10.1016/j.ocemod.2008.08.004.
- 25 Eyring, V., Bony, S., Meehl, G. A., Senior, C. A., Stevens, B., Stouffer, R. J., and K. E. Taylor (2016). Overview of the Coupled Model Intercomparison Project Phase 6 (CMIP6) experimental design and organization, *Geosci. Model Dev.*, 9, 1937–1958, doi:10.5194/gmd-9-1937-2016.
- Farneti, R., and P. R. Gent (2011). The effects of the eddy-induced advection coefficient in a coarse-resolution coupled climate model, *Ocean Modelling*, 39, 135–145, doi: 10.1016/j.ocemod.2011.02.005.
- 30 Frants, M., Holzer, M., DeVries, T., and R. Matear (2016). Constraints on the global marine iron cycle from a simple inverse model, *J. Geophys. Res. Biogeosci.*, 121, 28–51, doi: 10.1002/2015JG003111.
- Frenger, I., N. Gruber, R. Knutti and M. Münnich (2013). Imprint of Southern Ocean eddies on winds, clouds and rainfall. *Nature Geoscience*, 6(8), 608–612, doi: 10.1038/ngeo1863.
- 35 Frölicher, T. L., J. L. Sarmiento, D. J. Paynter, J. P. Dunne, J. P. Krasting and M. Winton (2015). Dominance of the Southern Ocean in anthropogenic carbon and heat uptake in CMIP5 models. *J. Climate*, 28(2), 862–886, doi: 10.1175/JCLI-D-14-00117.1.



- Galbraith, E.D., A. Gnanadesikan, J. P. Dunne and M.R. Hiscock (2010). Regional impacts of iron-light colimitation in a global biogeochemical model, *Biogeosciences*, 7, 1043–1064, doi: 10.5194/bg-7-1043-2010.
- Garcia, H.E., R.A. Locarnini, T.P. Boyer and J.I. Antonov (2010). World Ocean Atlas 2009, Volume 4: Nutrients (phosphate, nitrate, silicate). S. Levitus, Ed. NOAA Atlas NESDIS 71, U.S. Government Printing Office, Washington, D.C., 398 pp.
- 5 Garcia, H.E., R.A. Locarnini, T.P. Boyer and J.I. Antonov (2010). World Ocean Atlas 2009, Volume 3: Dissolved Oxygen, Apparent Oxygen Utilization, and Oxygen Saturation. S. Levitus, Ed. NOAA Atlas NESDIS 70, U.S. Government Printing Office, Washington, D.C., 344 pp.
- Gent, P. R. (2016). Effects of Southern Hemispheric Wind Changes on the Meridional Overturning Circulation in Ocean Models, *Annu. Rev. Mar. Sci.*, 8, 79–94, doi: 10.1146/annurev-marine-122414-033929.
- 10 Gent, P. R. and G. Danabasoglu (2011). Response to increasing Southern Hemisphere winds in CCSM4, *J. Climate*, 24(19), 4992–4998, doi: 10.1175/JCLI-D-10-05011.1.
- Gent, P. R. (2011). The Gent-McWilliams parameterization: 20/20 hindsight. *Ocean Modelling*, 39, 2–9, doi: 10.1016/j.ocemod.2010.08.002.
- Gent, P. R. and J. C. McWilliams (1990). Isopycnal mixing in ocean circulation models. *J. Phys. Oceanogr.*, 20, 150–155, doi: 10.1175/1520-0485(1990)020<0150:IMOCM>2.0.CO;2.
- 15 Gent, P. R., Willebrand, J., McDougall, T. J., and J. C. McWilliams (1995). Parameterizing eddy-induced tracer transports in ocean circulation models. *J. Physical Oceanography*, 25, 463–474, doi: 10.1175/1520-0485(1995)025<0463:PEITTI>2.0.CO;2.
- Getzlaff, J. and H. Dietze (2013). Effects of increased isopycnal diffusivity mimicking the unresolved equatorial intermediate current system in an earth system climate model. *Geophys. Res. Lett.*, 40, 2166–2170, doi: 10.1002/grl.50419.
- Getzlaff, J., Dietze, H. and A. Oschlies (2016). Simulated effects of southern hemispheric wind changes on the Pacific oxygen minimum zone. *Geophysical Research Letters*, 43, 2, 728–734, doi: 10.1002/2015GL066841.
- 20 Gnanadesikan, A., K.W. Dixon, S. M. Griffies, V. Balaji, M. Barreiro, J. A. Beesley, W. F. Cooke, T. L., Delworth, R. Gerdes, M. J. Harrison, I. M. Held, W. J. Hurlin, H. C. Lee, Z. Liang, G. Nong, R., C. Pacanowski, A. Rosati, J. Russell, B. L. Samuels, Q. Song, M. J. Spelman, R. J. Stouffer, C. O., Sweeney, G. Vecchi, M. Winton, A. T. Wittenberg, F. Zeng, R. Zhang, J. P. Dunne (2005). GFDL's CM2 Global Coupled Climate Models. Part II: The Baseline Ocean Simulation, *J. Climate*, 19, 675–697, doi: 10.1175/JCLI3629.1.
- 25 Griffies, S.M. A. Gnanadesikan, K. W. Dixon, J. P. Dunne, R. Gerdes, M. J. Harrison, A. Rosati, J. L. Russell, B. L. Samuels, M. J. Spelman, M. Winton and R. Zhang (2005). Formulation of an ocean model for global climate simulations. *Ocean Science* 1, 45–79, doi: 10.5194/os-1-45-2005.
- Hall, A., and M. Visbeck (2002). Synchronous variability in the Southern Hemisphere atmosphere, sea ice, and ocean resulting from the Annular Mode. *J. Climate*, 15(21), 3043–3057, doi: 10.1175/1520-0442(2002)015<3043:SVITSH>2.0.CO;2.
- 30 Hallberg, R. and A. Gnanadesikan (2006). The role of eddies in determining the structure and response of the wind-driven Southern Hemisphere overturning: Initial results from the Modelling Eddies in the Southern Ocean project, *J. Phys. Oceanogr.*, 36, 3312–3330, doi: 10.1175/JPO2980.1.
- Hogg, A. McC., M. P. Meredith, J. R. Blundell and C. Wilson (2008). Eddy heat flux in the Southern Ocean: Response to variable wind forcing. *J. Climate*, 21, 608–620, doi: 10.1175/2007JCLI1925.1.
- 35 Johnson, K. S., Gordon, R. M., and K. H. Coale (1997). What controls dissolved iron concentrations in the world ocean? *Marine Chemistry*, 57, 137–161, doi: 10.1016/S0304-4203(97)00043-1.
- Krishnamurthy, A., J.K. Moore, N. Mahowald, C. Luo, S.C. Doney, K. Lindsay and C.S. Zender (2009). Impacts of increasing anthropogenic soluble iron and nitrogen deposition on ocean biogeochemistry. *Glob. Biogeochem. Cycles*, 23, doi: 10.1029/2008GB003440.



- Large, W. G. and S. Yeager (2004). Diurnal to decadal global forcing for ocean and sea-ice models: the datasets and flux climatologies. NCAR Technical Note: NCAR/TN-460+STR, CGD Division of the National Centre for Atmospheric Research.
- Lenton, A. and R. J. Matear (2007). Role of the southern annular mode (SAM) in Southern Ocean CO₂ uptake. *Glob. Biogeochem. Cycles*, 21(2), doi: 10.1029/2006GB002714.
- 5 Lenton, A., B. Tilbrook, R. Law, D. C. Bakker, S. C. Doney, N. Gruber, M. Hoppema, M. Ishii, N. S. Lovenduski, R. J. Matear, B. I. McNeil, N. Metzl, S. E. Mikaloff Fletcher, P. Monteiro, C. Rödenbeck, C. Sweeney and T. Takahashi (2013). Sea-air CO₂ fluxes in the Southern Ocean for the period 1990-2009. *Biogeosciences*, 10, 4037–4054, doi: 10.5194/bg-10-4037-2013.
- Le Quéré, C., T. Takahashi, E. T. Buitenhuis, C. Rödenbeck and S. C. Sutherland (2007). Saturation of the Southern Ocean CO₂ sink due to recent climate change, *Science*, 316, 1735–1738, doi: 10.1126/science.1136188.
- 10 Locarnini, R.A., A.V. Mishonov, J.I. Antonov, T.P. Boyer and H.E. Garcia (2010). World Ocean Atlas 2009, Volume 1: Temperature. S. Levitus, Ed. NOAA Atlas NESDIS 68, U.S. Government Printing Office, Washington, D.C., 184 pp.
- Löptien, U. and H. Dietze (2015). Constraining parameters in marine pelagic ecosystem models - is it actually feasible with typical observations of standing stocks? *Ocean Science*, 11 (4), 573–590. doi: 10.5194/os-11-573-2015.
- Lovenduski, N. S., N. Gruber, S. C. Doney and I. D. Lima (2007). Enhanced CO₂ outgassing in the Southern Ocean from a positive phase of the Southern Annular Mode. *Glob. Biogeochem. Cycles*, 21(2), doi: 10.1029/2006GB002900.
- 15 Lovenduski, N. S., N. Gruber and S.C. Doney, (2008). Toward a mechanistic understanding of the decadal trends in the Southern Ocean carbon sink, *Glob. Biogeochem. Cycles*, 22, doi: 10.1029/2007GB003139.
- Lovenduski, N.S., M. C. Long, P. R. Gent and K. Lindsay (2013). Multi-decadal trends in the advection and mixing of natural carbon in the Southern Ocean, *Geophys. Res. Lett.*, 40, doi: 10.1029/2012GL054483.
- 20 Lovenduski, N. S., McKinley, G. A., Fay, A. R., Lindsay, K., and M. C. Long (2016). Partitioning uncertainty in ocean carbon uptake projections: Internal variability, emission scenario, and model structure. *Glob. Biogeochem. Cycles*, 30, doi: 10.1002/2016GB005426.
- Mahowald, N.M., S. Kloster, S. Engelstaedter, J.K. Moore, S. Mukhopadhyay, J.R. McConnell, S. Albani, S.C. Doney, A. Bhattacharya, M.A.J. Curran, M.G. Flanner, F.M. Hoffman, D.M. Lawrence, K. Lindsay, P.A. Mayewski, J. Neff, D. Rothenberg, E. Thomas, P.E. Thornton and C.S. Zender (2010). Observed 20th century desert dust variability: impact on climate and biogeochemistry, *Atmospheric Chemistry and Physics*, 10, doi:10.5194/acp-10-10875-2010.
- 25 Marshall, G. J. (2003). Trends in the Southern Annular Mode from observations and reanalyses. *J. Climate*, 16(24), 4134–4143, doi: 10.1175/1520-0442(2003)016<4134:TITSAM>2.0.CO;2.
- Marshall, J. and K. Speer, (2012). Closure of the meridional overturning circulation through Southern Ocean upwelling. *Nature Geoscience*, 5(3), 171–180, doi: 10.1038/ngeo1391.
- 30 McDougall, T. J. and J. A. Church (1985). Pitfalls with the Numerical Representation of Isopycnal and Diapycnal Mixing. *J. Physical Oceanography*, 16, 196–199, doi: 10.1175/1520-0485(1986)016<0196:PWTNRO>2.0.CO;2.
- Metzl, N. (2009). Decadal increase of oceanic carbon dioxide in Southern Indian Ocean surface waters (1991- 2007), *Deep-Sea Res. II*, 56, 607–619, doi: 10.1016/j.dsr2.2008.12.007.
- Rayner, N. A., D. P. Parker, E. B. Horton, C. K. Folland, L. V. Alexander, D. P. Rowell, E. C. Kent and A. Kaplan (2003). Global analyses of sea surface temperature, sea ice, and night marine air temperature since the late nineteenth century, *J. Geophys. Res.*, 108, D14, doi:10.1029/2002JD002670.
- 35 Resing, J. A., Sedwick, P. N., German, C. R., Jenkins, W. J., Moffett, J. W., Sohst, B. M., and A. Tagliabue (2015). Basin-scale transports of hydrothermal dissolved metals across the South Pacific Ocean, *Nature*, 523, 200–203, doi: 10.1038/nature14577.



- Smetacek, V., Klaas, C., Strass, V. H., Assmy, P., Montresor, M., Cisewski, B., Savoye, N., Webb, A., d'Ovidio, F., Arrieta, J. M., Bathmann, U., Bellerby, R., Berg, G. M., Croot, P., Gonzalez, S., Henjes, J., Herndl, G. J., Hoffmann, L. J., Leach, H., Losch, M., Mills, M. M., Neill, C., Peeken, I., Röttgers, R., Sachs, O., Sauter, E., Schmidt, M. M., Schwarz, J., Terbrüggen, A., and D. Wolf-Gladrow (2012). Deep carbon export from a Southern Ocean iron-fertilized diatom bloom, *Nature*, 487, 313–319, doi: 10.1038/nature11229.
- 5 Olgun, N., Duggen, S., Croot, P. L., Delmelle, P., Dietze, H., Schacht, U., Oskarsson, N., Siebe, C., Auer, A., and D. Garbe-Schönberg (2011). The role of airborne volcanic ash from subduction zone and hot spot volcanoes and related iron fluxes into the Pacific Ocean. *Glob. Biogeochem. Cycles*, 25, 1–15, doi: 10.1029/2009GB003761.
- Orr, J. C., Najjar, R. G., Aumont, O., Bopp, L., Bullister, J. L., Danabasoglu, G., Doney, S. C., Dunne, J. P., Dutay, J.-C., Graven, H., Griffies, S. M., John, J. G., Joos, F., Levin, I., Lindsay, K., Matear, R. J., McKinley, G. A., Mouchet, A., Oschlies, A., Romanou, A., Schlitzer, R., Tagliabue, A., Tanuha, T., and A. Yool (2016). Biogeochemical protocols and diagnostics for the CMIP6 Ocean Model Intercomparison Project (OMIP), *Geosci. Model Dev. Discussion*, doi: 10.5194/gmd-2016-155, 2016.10.5194/gmd-2016-155
- 10 Redi, M. H. (1982). Oceanic isopycnal mixing by coordinate rotation. *J. Physical Oceanography*, 12, 1154–1158, doi: 10.1175/1520-0485(1982)012<1154:OIMBCR>2.0.CO;2.
- Saenko, O. A., J. C. Fyfe and M. H. England (2005). On the response of the oceanic wind-driven circulation to atmospheric CO₂ increase. *Climate dynamics*, 25(4), 415–426, doi: 10.1007/s00382-005-0032-5
- 15 Screen, J. A., Gillett, N. G., Stevens, D. P., Marshall, G. J., and H. K. Roscoe (2009). The role of eddies in the Southern Ocean temperature response to the Southern Annular Mode, *J. Climate*, 22, 806–818, doi: 10.1175/2008JCLI2416.1.
- Sigman, D. M. and E.A. Boyle (2000). Glacial/interglacial variations in atmospheric carbon dioxide, *Nature*, 407(6806), 859–869, doi: 10.1038/35038000.
- 20 Simpkins, G. R. and A. Y. Karpechko (2012). Sensitivity of the southern annular mode to greenhouse gas emission scenarios, *Climate dynamics*, 38(3-4), 563–572, doi: 10.1007/s00382-011-1121-2.
- Smith, S.L., Yamanaka, Y., Pahlow, M. and A. Oschlies (2009). Optimal uptake kinetics: physiological acclimation explains the pattern of nitrate uptake by phytoplankton in the ocean, *Marine Ecology Progress Series*, 384, doi: 10.3354/meps08022.
- Tagliabue, A., Aumont, O., and L. Bopp (2014). The impact of different external sources of iron on the global carbon cycle, *Geophys. Res. Lett.*, 41, 920–926, doi: 10.1002/2013GL059059.
- 25 Tagliabue, A., Aumont, O., DeAth, R., Dunne, J. D., Dutkiewicz, S., Galbraith, E., Misumi, K., Moore, J. K., Ridgwell, A., Sherman, E., Stock, C., Vichi, M., Völker, C., and A. Yool (2016). How well do global ocean biogeochemistry models simulate dissolved iron distributions? *Glob. Biogeochem. Cycles*, 30, 149–174, doi: 10.1002/2015GB005289.
- Takahashi, T., S. C. Sutherland, R. Wanninkhof, C. Sweeney, R. A. Feely, D. W. Chipman, B. Hales, G. Friederich, F. Chavez, C. Sabine, A. Watson, D. C. E. Bakker, U. Schuster, N. Metzl, H. Yoshikawa-Inoue, M. Ishii, T. Midorikawa, Y. Nojiri, A. Kortzinger, T. Steinhoff, M. Hoppema, J. Olafsson, T. S. Arnarson, B. Tilbrook, T. Johannessen, A. Olsen, R. Bellerby, C. S. Wong, B. Delille, N. R. Bates, H. J. W. De Baar (2009). Climatological mean and decadal change in surface ocean pCO₂, and net sea-air CO₂ flux over the global oceans. *Deep-Sea Res. II: Topical Studies in Oceanography*, 56(8), 554–577, doi: 10.1016/j.dsr2.2008.12.009.
- 30 Thompson, D. W. L., and S. Solomon (2002). Interpretation of recent Southern Hemisphere climate change, *Science*, 296, 895–899, doi: 10.1126/science.1069270.
- 35 Verdy, A., S. Dutkiewicz, M. J. Follows, J. Marshall and A. Czaja (2007). Carbon dioxide and oxygen fluxes in the Southern Ocean: Mechanisms of interannual variability, *Glob. Biogeochem. Cycles*, 21, doi: 10.1029/2006GB002916.



- Veronis, G. (1975). The role of models in tracer studies. In: Numerical Models of the Ocean Circulation, R.O. Reid (ed), National Academy of Science, Washington, DC, pp. 133–146.
- Viebahn, J. and C. Eden (2010). Towards the impact of eddies an the response of the Southern Ocean to climate change, Ocean Modelling, 34, 150–165, doi: 10.1016/j.ocemod.2010.05.005.
- 5 Völker, C., and A. Tagliabue, (2015). Modeling organic iron-binding ligands in a three-dimensional biogeochemical ocean model, Marine Chemistry, 173, 67–77, doi: 10.1016/j.marchem.2014.11.008.
- Zickfeld, K., J. C. Fyfe, O. A. Saenko, M. Eby and A. J. Weaver (2007). Response of the global carbon cycle to human-induced changes in Southern Hemisphere winds. Geophys. Res. Lett., 34(12), doi: 10.1029/2006GL028797.

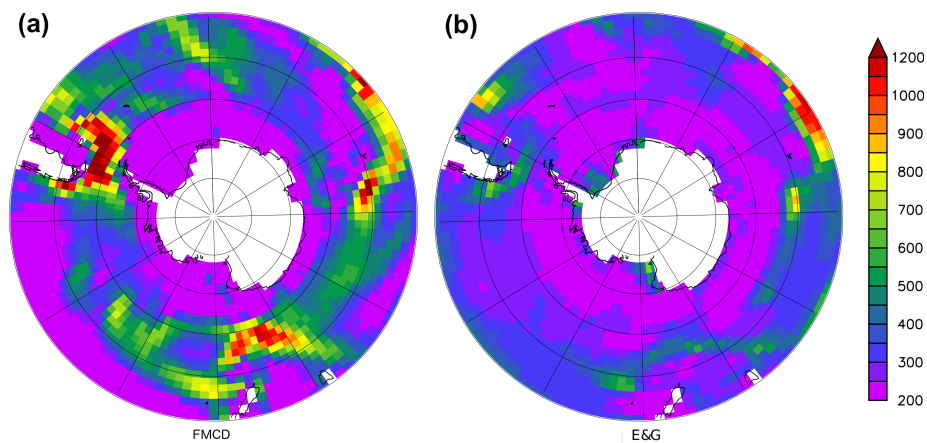


Figure 1. Vertical mean thickness diffusivities (upper 500 m), averaged over the last 20 years of spin-up. Subpanel (a) refers to configuration FMCD and (b) refers to configuration E&G. The units are $\text{m}^2 \text{s}^{-1}$.

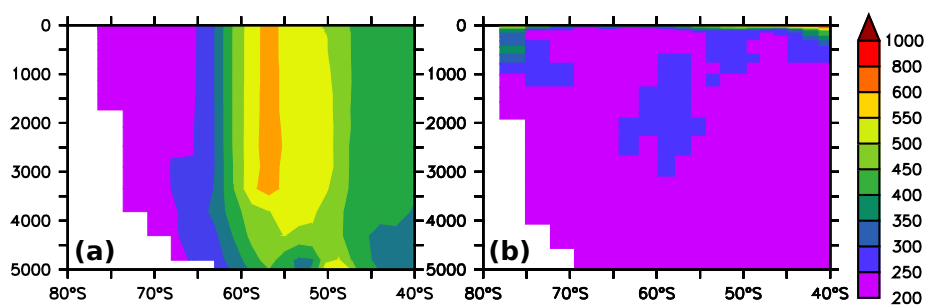


Figure 2. Zonal mean thickness diffusivities, averaged over the last 20 years of spin-up. Subpanels (a) and (b) refer to configuration FMCD and E&G, respectively. The units are $\text{m}^2 \text{s}^{-1}$.

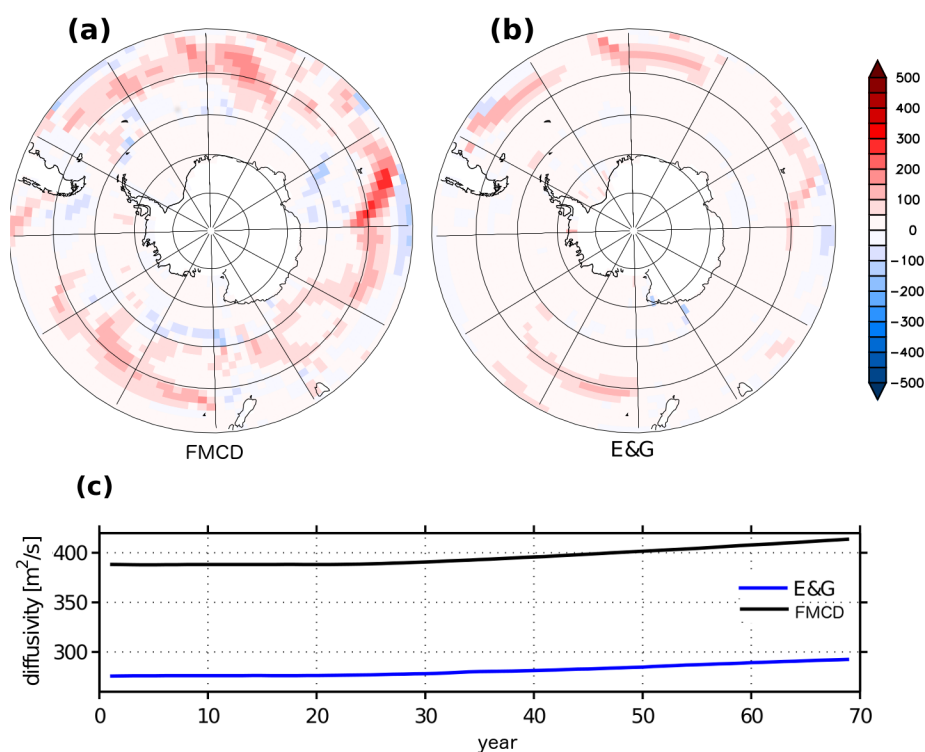


Figure 3. Temporal evolution of thickness diffusivity, average over the upper 1000 m. (a) and (b) refer to changes (the average of year 45–49 minus the average over the last 20 years of the spin-up) effected by increasing winds in simulation FMCD and E&G, respectively. (c) shows the evolution of the domain-averaged (south of 40°S) diffusivity simulated with FMCD (black line) and E&G (blue line). The first 20 years correspond to the end of respective spin-ups. From year 20 onward, the winds increase. The units are $\text{m}^2 \text{s}^{-1}$. Configuration CON (with a constant $600 \text{ m}^2 \text{s}^{-1}$) is not shown.

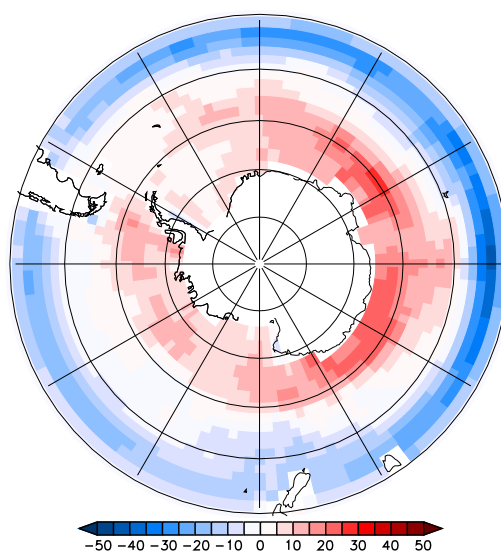


Figure 4. Acceleration of Ekman pumping as simulated with configuration FMCD (and IRON). The unit is m yr^{-1} . Regions with increased upwelling (or reduced pumping) are coloured in red.

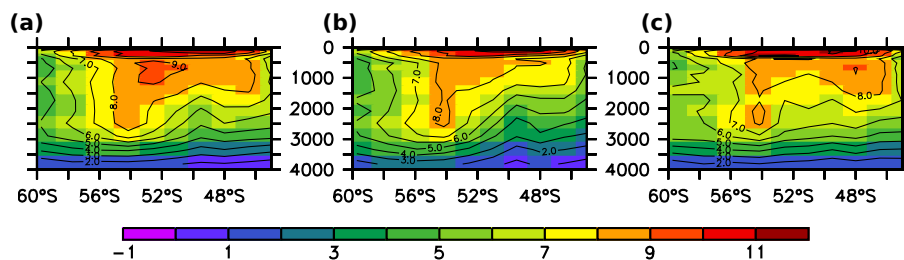


Figure 5. Change in meridional overturning (after 49 years of increasing winds) in units Sv ($10^6 \text{ m}^3 \text{ s}^{-1}$). Positive values indicate increasing overturning in response to increasing winds. (a), (b) and (c) refer to simulations CON, FMCD and E&G, respectively.

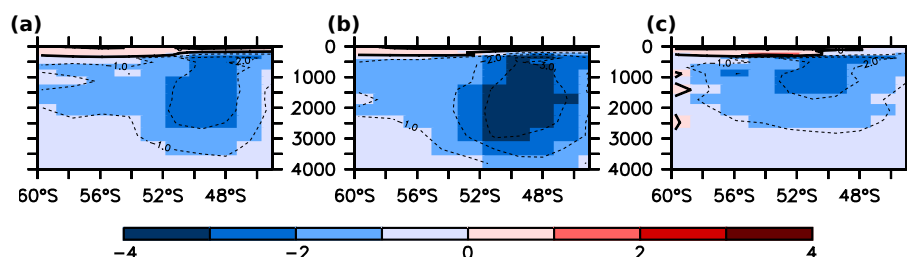


Figure 6. Change of that fraction of the meridional overturning that is effected by the respective GM parameterizations (after 49 years of increasing winds) in units Sv ($10^6 \text{ m}^3 \text{ s}^{-1}$). Negative values indicate a damping of the overturning in response to increasing winds. (a), (b) and (c) refer to simulations CON, FMCD and E&G, respectively.

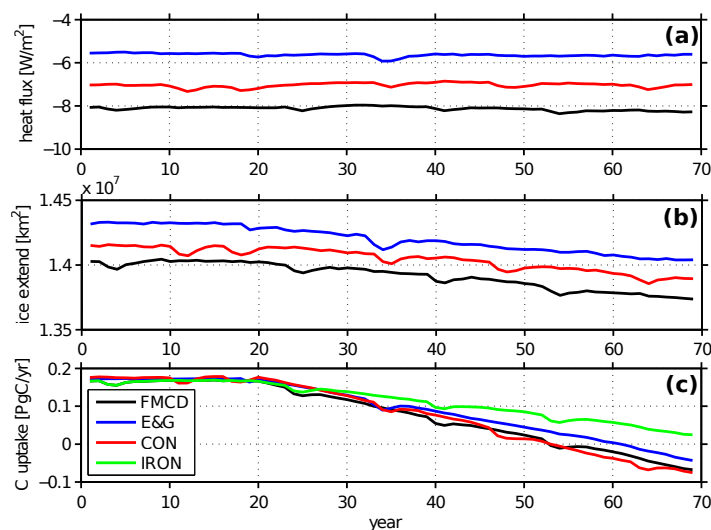


Figure 7. Oceanic response to increasing winds south of 40°S (spatially and annually averaged). (a) shows air-sea heat fluxes with negative values denoting oceanic cooling), (b) shows ice-covered area and (c) shows oceanic carbon uptake with positive values denoting oceanic uptake. The line colors refer to experiments as indicated in the legend. The first 20 years correspond to the end of respective spin-ups. From year 20 onward, the winds increase.

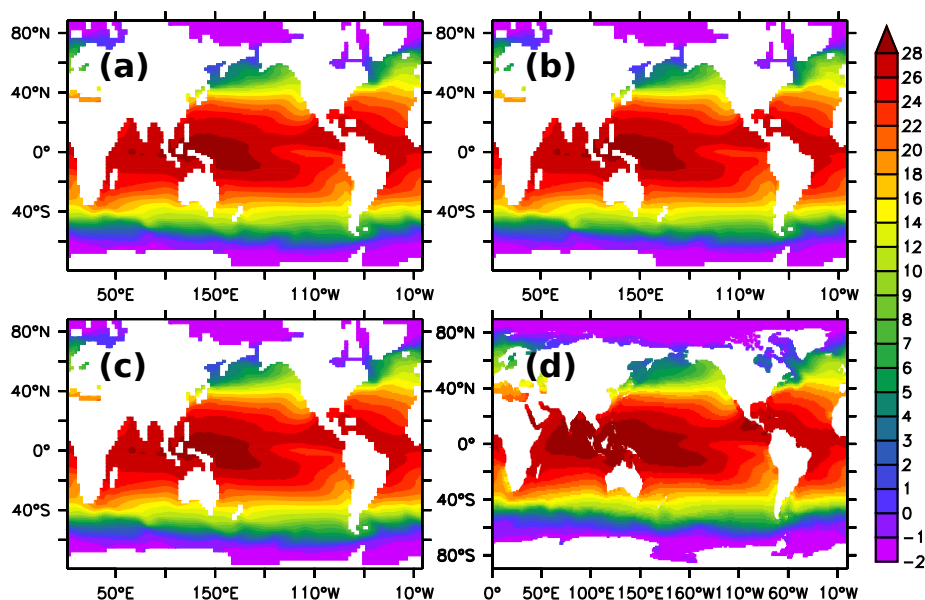


Figure 8. Annual mean sea surface temperature in units °C. (a), (b) and (c) refer to spun-up states of configurations FMCD, CON and E&G, respectively. (d) shows observations (Locarnini et al., 2010).

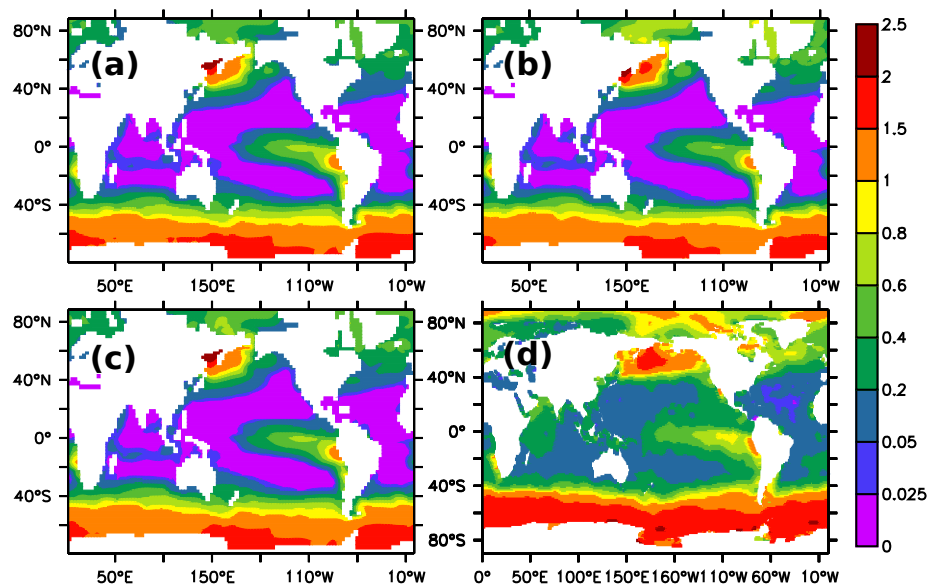


Figure 9. Annual mean surface phosphate concentration in units mmol P m^{-3} . The colour scale is nonlinear and highlights low, limiting concentrations. (a), (b) and (c) refer to simulations FMCD, CON and E&G, respectively. (d) shows observations (Garcia et al., 2010a).

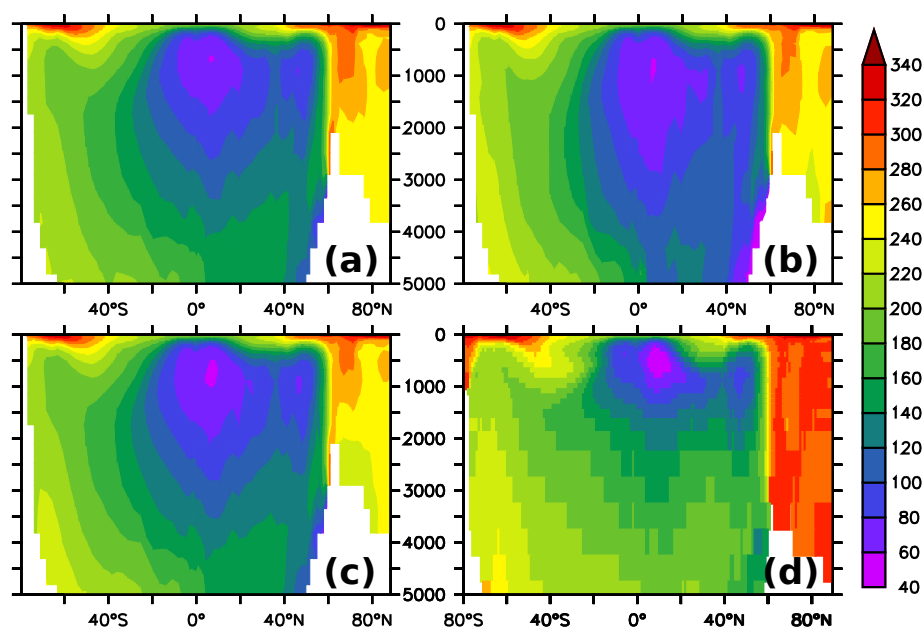


Figure 10. Meridional section of annual mean oxygen concentration in units $\text{mmol O}_2 \text{ m}^{-3}$ (zonally averaged). (a), (b) and (c) refer to simulations FMCD, CON and E&G, respectively. (d) shows observations (Garcia et al., 2010b).

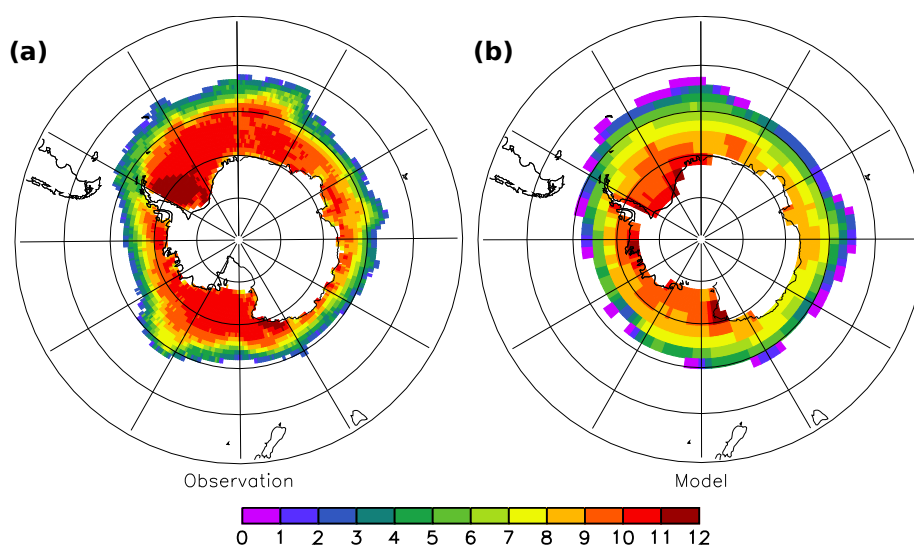


Figure 11. Ice covered months in a year. (a) refers to a 1990 to 2000 average derived from the Rayner et al. (2003) global analysis. (b) refers to the simulation FMCD.